Chip-scale atomic devices at NIST

Svenja Knappe[a], Peter Schwindt[a], Vladislav Gerginov[b], Vishal Shah[c], Alan Brannon[c], Brad Lindseth[c], Li-Anne Liew[c], Hugh Robinson[a], John Moreland[a], Zoya Popovic[c], Leo Hollberg[a], John Kitching[a]

[a]NIST, 325 Broadway, Boulder CO, USA, 80205
[b]University of Notre Dame, Notre Dame IN, USA 46556
[c]University of Colorado, Boulder CO, USA 80309

ABSTRACT

We provide an overview of our research on chip-scale atomic devices. By miniaturizing optical setups based on precision spectroscopy, we have developed small atomic sensors and atomic references such as atomic clocks, atomic magnetometers, and optical wavelength references. We have integrated microfabricated alkali vapor cells with small low-power lasers, micro-optics, and low-power microwave oscillators. As a result, we anticipate that atomic stability can be achieved with small size, low cost, battery-operated devices. Advances in fabrication methods and performance are presented.

Keywords: Atomic clocks, atomic magnetometers, coherent population trapping, CSAC, CSAM, laser spectroscopy, MEMS, microfabrication, vapor cells

1. INTRODUCTION

It has been shown that atoms can be used as sensors for a variety of parameters such as: time[1], magnetic fields[2,3], rotation[4], acceleration[5], RF power[6]. Some of the most precise sensors to date are based on precision laser spectroscopy of atoms. For many sensor applications, however, size, weight, power consumption, robustness, and price are of major importance, limiting the use of these sensors in everyday instruments.

Combining laser and atomic physics with microelectromechanical systems (MEMS) could benefit such applications. Enhanced precision or accuracy of atomic stabilization could be combined with wafer-level fabrication processes to reduce size, cost, and power consumption.

2. CELL FABRICATION

By developing a technique to make microfabricated alkali vapor cells[7], we have overcome one main obstacle for the development of chip-scale atomic sensors. The cell confines the atoms and provides access for the laser light. Furthermore, contamination of the cell has to be prevented, as alkali atoms are chemically reactive with many substances and their energy levels can be easily perturbed. Conventionally, alkali vapor cells have been made individually by use of glass-blowing techniques, which can make them expensive, bulky, and difficult to reproduce exactly.

MEMS fabrication techniques can drastically change the way alkali vapor cells are made and could therefore open up new avenues for their use. One of the simplest methods uses silicon wafers with an array of holes etched through them[7]. Two wafers of glass are anodically bonded[8] to both sides of the silicon, creating small cavities, each with two windows for optical access. While many cell fabrication approaches follow this concept, the deposition of alkali metal into the cavity can vary dramatically.

In some approaches, cesium metal has been inserted into the cell preforms with small-volume pipettes inside a glove box or an anaerobic chamber[7,9,10]. The cells were then bonded under a buffer-gas atmosphere of nitrogen and/or argon. With this method, care must be taken to ensure a controlled atmosphere inside the chamber in order to avoid excessive oxidized cesium inside the cell cavity. Furthermore, it can be difficult to ensure that no cesium gets deposited onto the silicon wafer, preventing it from interfering with the bonding process.

The latter problem can be prevented by use of a different approach, where a chemical mixture of salts is deposited into the cell cavity[11]. The pure alkali metal is them created through a chemical reaction between barium azide and alkali chloride that is thermally initiated during the bonding process. The advantages of this method are the possibility of producing small amounts of alkalis and that isotopically enriched alkali salts are available. A disadvantage, however, is the possibility of a reverse reaction, if the chemical compounds remain inside the cell. It has been found that nitrogen in a microfabricated cesium cell can be depleted form the background gas at a rate of 30 Pa/day[12]. This method is therefore not useful for devices measuring the hyperfine splitting, as it depends on the buffer gas pressure. Also, it will be very difficult to make vapor cells without any nitrogen using this technique.

Therefore, we have developed a method that does not leave remainders inside the cell cavity after bonding[12]. Here, the same reaction is started inside a small glass ampoule instead of the cell cavity, and the alkali atoms are evaporated through a glass nozzle of length ~5 mm and diameter 700 μm. This technique allows to separately choose and mix the alkali isotopes, the amount of alkali atoms inside the cell, and the combination and pressures of buffer gases.

Recently, a new method has been developed at NIST with the goal of wafer-level filling of cesium cells[13]. With the evaporative deposition of CsN_3 into the cell cavities through a shadow mask, it is based purely on MEMS processes. The cells are then anodically bonded under vacuum. Afterwards, the cesium is released by ultraviolet dissociation of the azide into cesium and nitrogen. This scheme has the potential of being able to batch fabricate large wafers of cells at the wafer level and at low cost.

Other groups have developed different methods to seal the alkali atoms inside the cell, either by sealing them in wax micropackets and releasing them into the cavity by melting the wax with a laser beam[14], or by diffusing them out of glass pieces at high temperatures[15]. Recently, cells have even been made using MEMS glass blowing methods[16].

3. CHIP-SCALE ATOMIC CLOCKS

By integrating these cells with vertical-cavity surface-emitting lasers (VCSELs) and microoptics components, we have miniaturized simple spectroscopic setups to volumes around 10 mm^3. All-optical excitation schemes[17] can be favorable because of their simplicity and easy confinement of the field at the point of the alkali atoms.

Figure 1c shows an example of such miniaturized precision spectroscopy setup, in this case designed as a chip-scale atomic clock (CSAC)[18] based on coherent population trapping (CPT)[19]. When the laser is modulated at exactly half the ground-state hyperfine splitting of the ^{87}Rb atoms, i.e., at 3.417 GHz, a ground-state coherence is created in the atoms that is out of phase with the driving light fields, and the absorption decreases. This resonance can be used to stabilize to the atomic transition the oscillator that generates the microwaves.

The CSAC physics package in Figure 1c consists of several layers of silicon and glass, and electrical connections are made through gold wire bonds to the glass baseplate. A VCSEL is placed on the bottom of the structure onto a resistive heater, and emits vertically. Light of wavelength 795 nm then passes through thermal isolation spacers, neutral density filters, a polarizer, and a quarter waveplate before interacting with the ^{87}Rb vapor inside a MEMS cell of 1 mm^3 interior volume. The cell is heated to ~ 90 °C by two transparent heaters directly placed above and below it. The transmitted laser light is detected by a photodiode on top of the cell.

The physics package takes as its input the 3.417 GHz signal of a miniature low-power voltage-controlled oscillator[20] (VCO) (Figure 1b), in this case integrated on the same baseplate (Figure 1a). It creates a DC output signal proportional to the frequency difference between the atomic $m_F = 0$ ground states and the VCO. A miniature electronic servo loop stabilizes the VCO frequency to the one given by the atoms. Furthermore, the control electronics stabilize the laser wavelength to the center of the optical atomic resonance and control the cell and VCSEL temperatures. Figure 2 is a schematic of the interactions between the major subsystems of the clock.

The integrated physics board[21] operated with rack-sized electronics reached a frequency stability of $1.5 \times 10^{-10}/\tau^{-1/2}$. This was limited mainly by the frequency noise of the VCSEL and the phase noise of the low-power VCO. Short-term

instabilities as low as $4.5 \times 10^{-11}/\tau^{-1/2}$ have been measured in CSAC physics packages with different VCSELs and large synthesizers[22].

We have integrated such a physics board containing a physics package and a low-power VCO[20,21] with small control electronics into a fully-functional CSAC. In a volume of 15 cm^3, it reached a fractional frequency instability in the 10^{-10} range at averaging times between 15 seconds and several hours. The total power consumption was 300 mW. Other groups have demonstrated complete CSACs with much better thermal design[9] consuming less than 110 mW of power[23], with half of the power consumed by a commercial 4.6 GHz VCO.
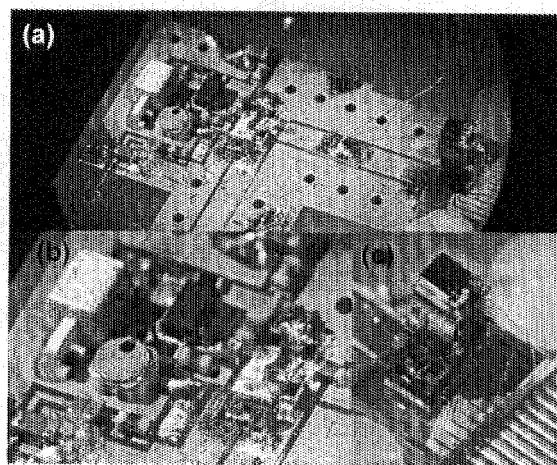

Figure 1(a) Photograph of the physics board containing a 3.4 GHz VCO integrated with a CSAC physics package. Inputs are the DC bias and tune voltage for the VCO and the laser bias, the photodetector bias, and the heater currents for the physics package. Outputs are stabilized 3.4 GHz and diagnostic signals. (b) Closeup view of the VCO and (c) the physics package.

One of the major problems with the frequency stability is the large tunability of the VCSEL with temperature. Small temperature gradients between thermistor and VCSEL over a distance of a few hundred micrometers can lead to frequency shifts of around 45 Hz/K. This can be prevented by stabilizing the laser and cell temperature (in addition to the laser and VCO frequencies) to signals derived only from the atoms[24]. Furthermore, the requirements on the laser frequency noise and stabilization of the VCSEL could be relaxed when implementing more advanced spectroscopic setups[25].
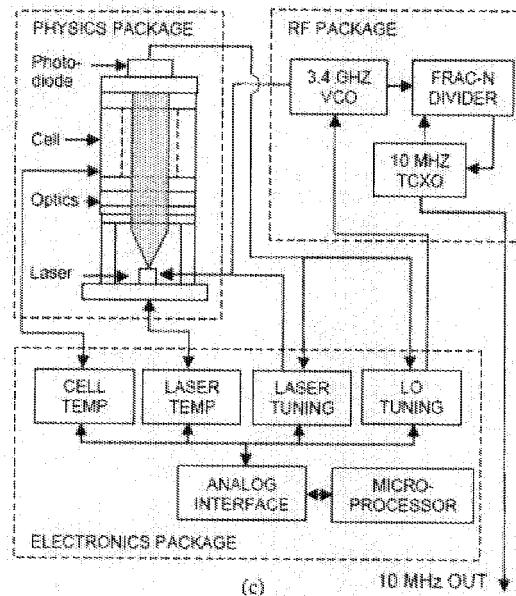
Figure 2 Schematic indicating major CSAC subsystems and interconnects

4. CHIP-SCALE ATOMIC MAGNETOMETERS

Similar vapor cells have been used to build physics packages of atomic magnetometers based on CPT[26] and spin precession[2]. A CPT magnetometer works in a way similar to that of the chip-scale clock. The frequency splitting between two ground-state hyperfine components is measured. For the clock, the $m_F = 0$ Zeeman sublevels were chosen because of their reduced sensitivity to magnetic fields. In the chip-scale magnetometer, Zeeman components with high frequency shifts in magnetic fields are favored. This specific CPT magnetometer used the $m_F = +1$ Zeeman sublevels in a longitudinal magnetic field, although transitions in a transverse field can also be used[27]. Sensitivities around 50 pT/Hz$^{1/2}$ at 10 Hz have been reached[28] in a sensor volume of 1 mm^3. The physics package looked very similar to the one in Figure 1c. The bandwidth of this device was limited to below 100 Hz because of the large magnetic field gradient across the cell volume generated by the cell heaters. The heating current was therefore chopped and a sample-and hold circuit ensured measurement only when the current was off.

In order to determine the total magnetic field, the frequency of the magnetically sensitive transition has to be compared to the frequency of the clock transition. This requires either frequent recalibration, or tight control of frequency drifts. Of major concern here are temperature-induced drifts due to buffer-gas collisions in the cell and light shifts. The first shift requires a precise control of the ratio of different buffer gasses in order to minimize the temperature coefficient. This can be especially difficult to do in a MEMS cell, where sealing is performed above 300 °C and the mechanisms of anodic bonding are not well understood yet.

The sensitivity of the hyperfine magnetometer is limited also by the maximum possible buffer gas pressure. While the buffer gas broadens the ground states only weakly, the excited P-states broaden with a rate of around 2 MHz/kPa for nitrogen and argon[29]. If the broadening of the excited states becomes similar to the modulation frequency of the VCSEL the amplitude of the CPT resonance is reduced, because of single-photon transitions from the other modulation sidebands and different phases between the beatnotes of the "resonant" and "non-resonant" sidebands of the frequency modulated VCSEL[30]. This limits the nitrogen pressure to below 20 kPa. At such a pressure, the CPT linewidth in a 1 mm cell is still limited by collisions of the alkali atoms with the walls[1,31].
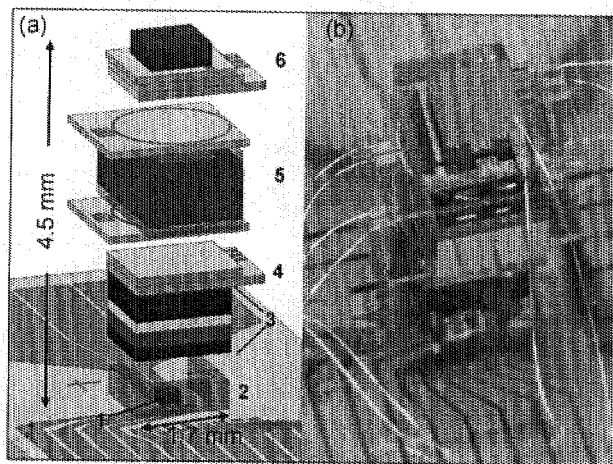
Figure 3 The chip-scale atomic magnetometer. (a) Schematic of the magnetic sensor. The components are: 1-VCSEL; 2-polyimide spacer; 3-optics package including (from bottom to top) a neutral-density filter, polarizer, a quartz λ/4 waveplate, and a neutral-density filter; 4-ITO heater; 5-[87]Rb vapor cell with RF coils above and below it; and 6- ITO heater and photodiode assembly. (b) Photograph of the magnetic sensor. Note the gold wire bonds providing the electrical connections from the base plate to device.

Better sensitivities of chip-scale atomic magnetometers have been reached when measuring the spin precession directly. Figure 3 shows a photograph and schematic of the physics package[32] of a magnetometer operating on the M_x technique[2,33]. Here, a resonant circularly polarized laser beam creates an atomic polarization that precesses around the external magnetic field at the Lamor frequency[34], i.e., 7 kHz/μT for [87]Rb, at random phase. When an RF field at the Lamor frequency is applied, it can make the atomic spins precess coherently in phase. This can be seen as a modulation of the absorbed light on a photodetector after the cell. The maximum sensitivity of the magnetometer is reached when the external magnetic field is at a 45° angle with respect to the propagation of the light field. Magnetic sensitivities around 6 pT/Hz$^{1/2}$ have been measured within a bandwidth between 1 Hz and 100 Hz. By implementing a new heater design with much reduced magnetic fields, the 3 dB bandwidth has been increased to 1 kHz.

In this magnetometer, a MEMS cell contains [87]Rb along with 270 kPa of nitrogen, which broadens the optical line to 18 GHz. With such high buffer gas pressures, the linewidth is no longer limited by wall collisions, but spin-exchange collisions are the major broadening mechanism. While the sensitivity of the magnetometer has been improved by using the spin precession resonance instead of the hyperfine resonance and the requirement of a microwave oscillator has been eliminated, one of the major systematic errors can now arise from the second-order Zeeman shift due to the interaction of the electrons with the nuclear magnetic moment.

5. MICROFABRICATED WAVELENGTH REFERENCE

Laser frequency stabilization has become an essential tool in many atomic physics experiments. Often, the frequency needs to be controlled to within less than 1 MHz, and sub-Doppler spectroscopy is used. One common method for sub-Doppler stabilization is saturated absorption spectroscopy[35]. As a first step towards a microfabricated wavelength reference, we have assembled a MEMS cell with microoptics components into a small saturated absorption spectroscopy unit, which could be used for laser frequency stabilization[36]. Figure 4 shows a photograph and schematic of such a setup. The laser beam from a distributed Bragg reflector (DBR) laser at 795 nm is split into pump and probe beam, by the first polarizing beam splitter. The pump beam passes through the vapor of natural rubidium and excites the atoms on the D$_1$ line. The counter-propagating probe beam has opposite Doppler shift for a moving atom and can therefore be absorbed

for all velocity classes except v = 0. The so-called Lamb dips and crossover resonances had widths around 35 MHz. In this setup, the two beams had orthogonal circular polarizations and the contrast of the dips of up to 40 % was due partly to optical pumping effects.
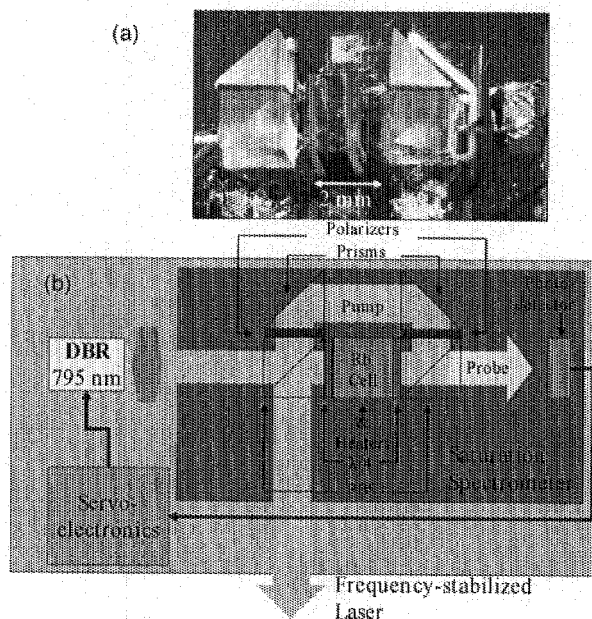

Figure 4 (a) Photograph of the microfabricated saturated absorption spectrometer setup. (b) Schematic of a stable wavelength reference including a laser locked to a stable sub-Doppler absorption resonance. **Dark Inset:** Schematic of the microfabricated setup, which consists of a vapor cell with two heaters, two polarizing beam splitters, two polarizers, two prisms, two quarter waveplates, and a photodetector.

The vapor cells containing the natural mixture of rubidium isotopes were of 1 mm length. They were heated with a transparent heater to ~45 °C to reach 30 % absorption. They were fabricated by the evaporation method, where care had to be taken that no gases remained inside the cell after bonding in order not to homogeneously broaden the optical lines. But at the same time, because no nitrogen is present to quench the optical fluorescence, and the path lengths of the miniaturized setup are only a few millimeters long, the fluorescence emitted by the alkali atoms can cause problems on the photodetector.

6. CONCLUSION

We described three examples of chip-scale atomic devices, based on precision laser spectroscopy in microfabricated vapor cells, where the synergism of laser and atomic physics with MEMS technology could open a whole new market for practical applications. Prototypes of completely integrated chip-scale atomic clocks have been made and tested, and developments to improve their performance are underway. Chip-scale atomic magnetometer physics packages based on hyperfine and Zeeman transitions have been demonstrated. Finally, one example of a sub-Doppler spectroscopic setup has been shown.

Different methods for cell fabrication have been introduced, depending on the specific application. MEMS cells with alkali atoms such as Cs and ^{85}Rb and ^{87}Rb in various isotopical ratios have been made. The sizes of these cells can vary from several hundred micrometers to a few millimeters. Combinations of buffer gases such as nitrogen, argon, neon, hydrogen, and xenon have been made at pressures from 0.1 to 1000 kPa.

REFERENCES

1. J. Vanier and C. Audoin, *The Quantum Physics of Atomic Frequency Standards*. (Adam Hilger, Bristol and Philadelphia, 1989).
2. A.L. Bloom, "Principles of operation of the rubidium vapor magnetometer," Appl. Opt. 1, 61-68 (1962).
3. J. C. Allred, R. N. Lyman, T. W. Kornack, M.V. Romalis, "High-Sensitivity Atomic Magnetometer Unaffected by Spin-Exchange Relaxation," Phys. Rev. Lett. 89 (13), 130801 (2002).
4. J.C. Frazer, US (1963); T. L. Gustavson, P. Bouyer, and M. A. Kasevich, "Precision rotation measurements with an atom interferometer gyroscope," Phys. Rev. Lett. 78 (11), 2046-2049 (1997).
5. M. J. Snadden, J. M. McGuirk, P. Bouyer, K.G. Haritos, M.A. Kasevich, "Measurement of the Earth's Gravity Gradient with an Atom Interferometer-Based Gravity Gradiometer," Phys. Rev. Lett. 81 (5), 971-974 (1998).
6. J. C. Camparo, "Atomic Stabilization of Electromagnetic Field Strength Using Rabi Resonances," Phys. Rev. Lett. 80 (2), 222-225 (1998).
7. L. A. Liew, S. Knappe, J. Moreland H.G. Robinson, L.Hollberg,J. Kitching, "Microfabricated alkali atom vapor cells," Appl. Phys. Lett. 84 (14), 2694-2696 (2004).
8. G. Wallis and D. Pomerantz, "Field Assisted Glass-Metal Sealing," Journal of Applied Physics 40 (10), 3946-3949 (1969).
9. R. Lutwak, J. Deng, W. Riley et al., presented at the 36th Annual Precise Time and Time Interval (PTTI) Meeting, Washington, DC, 2004.
10. M.H. Kwakernaak, S. Lipp, S. McBride P. Zanzucchi, W.K. Chan, V.B. Khalfin, H. An, J.R.D. Whaley, B. I. Willner, A. Ulmer, J.Z. Li, T. Davis, A.M. Braun, J.H. Abeles, A. Post, Y.-Y. Jau, N.N. Kuzma, W. Happer, 36th Annual Precise Time and Time Interval (PTTI) Meeting, Washington, DC, 2004.
11. S. Knappe, V. Velichansky, H.G. Robinson, L. Liew, J. Moreland, J. Kitching, L. Hollberg, Proceedings of the 2003 IEEE International Frequency Control Symposium and PDA Exhibition Jointly with the 17th European Frequency and Time Forum, 2003.
12. S. Knappe, V. Gerginov, P.D.D. Schwindt, V. Shah,H. G. Robinson, L. Hollberg, J. Kitching, "Atomic vapor cells for chip-scale atomic clocks with improved long-term frequency stability," Opt. Lett. 30 (18), 2351-2353 (2005).
13. L. Liew, J. Moreland, and V. Gerginov, Proceedings of the 20th Eurosensors conference, Goteberg, Sweden, accepted, 2006.
14. S. Radhakrishnan and A. Lal, Digest of Technical Papers - International Conference on Solid State Sensors and Actuators and Microsystems, TRANSDUCERS '05, 2005.
15. F. Gong, Y. Y. Jau, K. Jensen, W. Happer, "Electrolytic fabrication of atomic clock cells," Rev. Sci. Instrum. 77 (7), 076101 (2006).
16. J. Erklund and A. Shkel, "Glass Blowing on Wafer Level," submitted to J. MEMS (2006).
17. N. Cyr, M. Tetu, and M. Breton, "All-Optical Microwave Frequency Standard - a Proposal," IEEE Trans. Instrum. Meas. 42 (2), 640-649 (1993); W.E. Bell and A.L. Bloom, "Optically driven spin precession," Phys. Rev. Lett. 6, 280 (1961).
18. S. Knappe, V. Shah, P. D. D. Schwindt, L. Hollberg, J. Kitching, L.-A. Liew, J. Moreland, "A microfabricated atomic clock," Appl. Phys. Lett. 85 (9), 1460-1462 (2004).
19. G. Alzetta, A. Gozzini, L. Moi, R.M. Celli, A. Rossi, "Experimental-Method for Observation of Rf Transitions and Laser Beat Resonances in Oriented Na Vapor," Nuovo Cimento Della Societa Italiana Di Fisica B-General Physics Relativity Astronomy and Mathematical Physics and Methods 36 (1), 5-20 (1976); E. Arimondo, in *Progress In Optics, Vol 35* (Elsevier Science Publ B V, Amsterdam, 1996), Vol. 35, pp. 257-354; J. Vanier, "Atomic clocks based on coherent population trapping: a review," Appl. Phys. B 81 (4), 421-442 (2005).
20. A. Brannon, J. Breitbarth, and Z. Popovic, 2005 IEEE MTT-S International Microwave Symposium, 2005.
21. A. Brannon, M. Janković, J. Breitbarth, Z. Popović, V. Gerginov, V. Shah, S. Knappe, L. Hollberg, J. Kitching, IEEE Frequency Control Symposium, Miami, FL, 2006, in print.
22. S. Knappe, P. D. D. Schwindt, V. Shah, L. Hollberg, J. Kitching, L.-A. Liew, J. Moreland, "A chip-scale atomic clock based on Rb-87 with improved frequency stability," Opt. Express 13 (4), 1249-1253 (2005).

23. R. Lutwak, P. Vlitas, M. Varghese, M. Mescher, D.K. Serkland, G.M. Peake, Joint Meeting of the IEEE International Frequency Control Symposium and the Precise Time and Time Interval (PTTI) Systems and Applications Meeting, Vancouver, Canada, 2005.

24. V. Gerginov, S. Knappe, V. Shah, L. Hollberg, J. Kitching, " Atomic-based stabilization for laser-pumped atomic clocks," Opt. Lett. **31** (12), 1851-1853 (2006).

25. M. Rosenbluh, V. Shah, S. Knappe, J. Kitching, "Differentially Detected Coherent Population Trapping Resonances Excited by Orthogonally Polarized Laser Fields," Opt. Express, **14**, 6588-6594 (2006); V. Gerginov, V. Shah, S. Knappe, L. Hollberg, J. Kitching, "Laser noise cancellation in single-cell CPT clocks," to be submitted.

26. M. Stähler, R. Wynands, S. Knappe, J. Kitching, L. Hollberg, A. Taichenachev, V. Yudin, "Coherent population trapping resonances in thermal Rb-85 vapor: D-1 versus D-2 line excitation," Opt. Lett. **27** (16), 1472-1474 (2002).

27. M. Stähler, S. Knappe, C. Affolderbach, W. Kemp, R. Wynands, "Picotesla magnetometry with coherent dark states," Europhys. Lett. **54** (3), 323-328 (2001).

28. P. D. D. Schwindt, S. Knappe, V. Shah, L. Hollberg, J. Kitching, L.-A. Liew, J. Moreland, "Chip-scale atomic magnetometer," Appl. Phys. Lett. **85** (26), 6409-6411 (2004).

29. N. Allard and J. Kielkopf, "The effect of neutral nonresonant collisions on atomic spectral lines," Rev. of Mod. Phys. **54** (4), 1103-1182 (1982).

30. A. B. Post, Y. Y. Jau, N. N. Kuzma, W. Happer, "Amplitude- versus frequency-modulated pumping light for coherent population trapping resonances at high buffer-gas pressure," Phys. Rev. A **72** (3), 1-17 (2005).

31. N. Beverini, P. Minguzzi, and F. Strumia, "Foreign-Gas-Induced Cesium Hyperfine Relaxation," Phys. Rev. A **4** (2), 550-555 (1971).

32. P. D. D. Schwindt, B. Lindseth, S. Knappe L. Hollberg, J. Kitching, L.-A. Liew, J. Moreland, "A chip-scale atomic magnetometer with improved sensitivity using the Mx technique," submitted to Appl. Phys. Lett. (2006).

33. S. Groeger, G. Bison, J. L. Schenker, R. Wynands, A. Weis, "A high-sensitivity laser-pumped Mx magnetometer," Eur. Phys. J. D **38** (2), 239-247 (2006); E.B. Alexandrov, M.V. Balabas, A.K. Vershovski, A.E. Ivanov, N.N. Yakobson, V.L. Velichanski, N.V. Senkov, "Laser pumping in the scheme of an Mx-magnetometer," Optics and. Spectroscopy **78**, 325-332 (1995).

34. H. Dehmelt, "Modulation of a light beam by precessing absorbing atoms," Phys. Rev. **105**, 1924-1925 (1957).

35. T. W. Hänsch, M. D. Levenson, and A. L. Schawlow, "Complete Hyperfine Structure of a Molecular Iodine Line," Phys. Rev. Lett. **26**, 946 (1971); K. B. Macadam, A. Steinbach, C. Wieman, "A Narrow-Band Tunable Diode-Laser System With Grating Feedback, And A Saturated Absorption Spectrometer For Cs And Rb," Am. J. Phys. **60** (12), 1098-1111 (1992).

36. S. Knappe, H.G. Robinson, and L. Hollberg, "Microfabricated Saturated Absorption Spectroscopy with Alkali Atoms," to be submitted.